LBL-34139
UC-402
Preprint

Lawrence Berkeley Laboratory

UNIVERSITY OF CALIFORNIA

ENERGY & ENVIRONMENT DIVISION

Submitted to Aerosol Science and Technology

Experimental Determination of ETS Particle Deposition in a Low Ventilation Room

M. Xu, M. Nematollahi, R.G. Sextro, A.J. Gadgil, and W.W. Nazaroff

May 1993

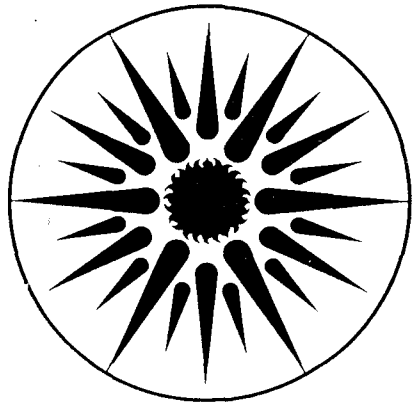

ENERGY & ENVIRONMENT DIVISION

Prepared for the U.S. Department of Energy under Contract Number DE-AC03-76SF00098

Submitted to Aerosol Science and Technology

LBL-34139
UC-402

Experimental Determination of ETS Particle Deposition in a Low Ventilation Room

Mindi Xu, Matty Nematollahi, Richard G. Sextro, and Ashok J. Gadgil
Indoor Environment Program
Lawrence Berkeley Laboratory
University of California
Berkeley, CA 94720

William W. Nazaroff
Department of Civil Engineering
University of California
Berkeley, CA 94720

May 1993

This work is supported by funds provided by the Cigarette and Tobacco Surtax Fund of the State of California through the Tobacco-Related Disease Research Program of the University of California, Grant Number 1RT299. This work was also supported by the Director, Office of Energy Research, Office of Health and Environmental Research, Physics and Technology Research Division of the U.S. Department of Energy, under Contract DE-AC03-76SF00098.

ABSTRACT

Deposition on indoor surfaces is an important removal mechanism for tobacco smoke particles. We report measurements of deposition rates of environmental tobacco smoke particles in a room-size chamber. The deposition rates were determined from the changes in measured concentrations by correcting for the effects of coagulation and ventilation. The air flow turbulent intensity parameter was determined independently by measuring the air velocities in the chamber. Particles with diameters smaller than

0.25 μm coagulate to form larger particles of sizes between 0.25-0.5 μm. The effect of coagulation on the particles larger than 0.5 μm was found to be negligible. Comparison between our measurements and calculations using Crump and Seinfeld's theory showed smaller measured deposition rates for particles from 0.1 to 0.3 μm in diameter and greater measured deposition rates for particles larger than 0.6 μm at three mixing intensities. Comparison of Nazaroff and Cass' model for natural convection flow showed good agreement with the measurements for particles larger than 0.1 μm in diameter; however, measured deposition rates exceeded model prediction by a factor of approximately four for particles in size range 0.05-0.1 μm diameter. These results were used to predict deposition of sidestream smoke particles on interior surfaces. Calculations predict that in 10 hours after smoking one cigarette, 22% of total sidestream particles by mass will deposit on interior surfaces at 0.03 air change per hour (ACH), 6% will deposit at 0.5 ACH, and 3% will deposit at 1 ACH.

INTRODUCTION

Environmental tobacco smoke (ETS) was recently recognized by EPA as a human carcinogen (US EPA, 1993). Available information indicates that ETS consists of many chemicals in particle and gas phases (National Research Council, 1986; Sexton et al., 1986; Benner et al., 1989; Eatough et al., 1989a, 1989b). Several of these chemicals are semi-volatile and appear in both phases. While the ETS gases and particles can be removed from the indoor air by deposition and ventilation, the deposited particles may continue to emit semi-volatile chemicals into the room air for a long time. The process of volatilization of particle phase nicotine is illustrated by a reported 80% loss of nicotine from spiked filters after sampling 200 liters of air (Badre et al., 1978). Due to the evaporation of deposited particles and the re-emission of adsorbed chemicals, a past smoking site may still exhibit a certain level of ETS constituents (Benner et al., 1989; Nelson et al., 1992; Turner et al., 1992). The odor that one experiences in a recently used smoking area is evidence of this evaporation and re-emission.

It is anticipated that the non-smoking family members of a smoker are not only exposed to a high concentration of ETS, which includes mainstream and sidestream smoke during smoking, but also to a lower concentration of ETS chemicals originating from the deposited particles and adsorbed chemicals. Constituted partly of mutagenic and carcinogenic substances and heavy metals (National Research Council, 1986; Sexton et al., 1986; Benner et al., 1989; Eatough et al., 1989a, 1989b), the deposited ETS particles may be ingested with food that has touched a contaminated surface. Ingestion of ETS residues may be more significant in children, where sucking or licking of fingers is common. Therefore, ETS particles removed from the air through deposition on interior surfaces may still pose some threat to human health.

Particle deposition depends on many parameters such as particle size, ventilation rate, air circulation, surface characteristics, and temperature difference between air and

surfaces (Crump and Seinfeld, 1981; Nazaroff and Cass, 1989a). Deposition of ETS particles has been studied in research chambers under controlled conditions (Offermann et al., 1985; Ingebrethsen and Sears, 1989). Deposition rate is usually determined indirectly by measuring aging concentrations of suspended particles (Crump et al., 1983; Offermann et al., 1985; McMurry and Grosjean, 1985; Okuyama et al., 1986; Pandian and Friedlander, 1988; Ingebrethsen and Sears, 1989; Chen et al., 1992). Ligocki et al. (1990) studied deposition by collecting particles on a carbon-coated substrate and analyzing the samples with a scanning electron microscope. This technique appears inappropriate for determining the deposition rates of ETS particles because of the particle evaporation during preparation of the samples (Ligocki et al., 1990; Nazaroff et al., 1990). ETS particle deposition has also been numerically simulated for different indoor conditions (Nazaroff and Cass, 1989a, 1989b). Nevertheless, more experimental measurements of ETS particle deposition in a room are necessary.

The work described in this paper was undertaken to determine ETS particle deposition in a room-size chamber. The experimental measurements, corrected for the effect of particle coagulation, were compared with theoretical predictions (Crump and Seinfeld, 1981; Nazaroff and Cass, 1989a). The size-segregated mass deposition of ETS particles has been estimated for the experimental room conditions.

EXPERIMENTS

The experiments were conducted at the Indoor Air Quality Research House (IAQRH) located at the Richmond Field Station of the University of California. A detailed description of IAQRH has been previously published (Offermann et al., 1985) and is briefly summarized here. Shown in Figure 1, the room used in this study is 4.56 m long, 3.38 m wide, and 2.37 m high. Its walls and ceiling are constructed of plasterboard and plywood and painted white. The floor is linoleum. The room is equipped with an exhaust hood and a HEPA filter air cleaner. The exhaust hood and the air cleaner are located close to two

corners. A smoking machine is located at the center of the room. The relative humidity and temperature probes are set near the room center and about 25 cm below the ceiling. A 7.6 cm. (3") muffin fan is installed near the center of each wall with the fan axis oriented horizontally and parallel to the wall. The fans are oriented to blow air towards two opposite corners of the room, as indicated in Figure 1. The aerosol instruments and data acquisition system are located in an adjacent room.

ETS Particle Generation

In each experimental trial, one Kentucky Reference cigarette 2R1 was machine smoked (Arthur D. Little, Model ADL II Smoking System) to generate ETS particles. The cigarette was ignited with a small coil of nichrome wire under computer control and smoked at the rate of one 35 cm^3 puff per minute. Combustion was terminated by snuffing the cigarette at a butt length of 30 mm using a motor-driven glass tube, sealed at one end, which was actuated as the cigarette burned through a trigger-thread. Mainstream smoke was exhausted to the outside through a plastic tube and sidestream smoke was emitted into the experimental room.

Particle Measurement

The ETS particles were sampled through a 3 m sample line of 0.95 cm ID (3/8") copper refrigeration tubing and a stainless steel manifold which distributed the flow to the aerosol measurement instruments. The sample in the manifold was continuously refreshed by using a pump to draw 2 LPM in excess of the instrument-driven flow through the manifold, which totaled 4.3 LPM. All of these flows were exhausted to the outside. A condensation nucleus counter (CNC) (TSI, Model 3020) was used to measure the total particle concentration. The size-segregated particle concentrations were measured with an optical particle counter (OPC) (Particle Measuring Systems, LAS-X) and a differential mobility particle sizer (DMPS), consisting of an electrostatic classifier (EC) (TSI, Model 3071) and an ultrafine condensation particle counter (UCPC) (TSI, Model 3025). The OPC counts particles in 16 size channels ranging in diameter from 0.09 to >3 μm. The

DMPS was operated to provide particle populations in 14 size channels with diameters from 0.01 to 0.35 μm.

The OPC was calibrated by the manufacturer with polystyrene latex (PSL) particles. ETS particle sizes reported by the OPC might be different from the true size due to the different refractive index (McRae, 1982). A preliminary calibration of the OPC with ETS particles was carried out before the experiments. The monodisperse aerosol outflow from the EC was sampled with the OPC at several particle sizes corresponding to the central region of each of the OPC's lower eight channels. The particle diameters reported by the OPC were then compared with the EC output size. A difference of about 0.03 μm was found by comparing the upper sizes of each OPC and EC output bin. This is similar to the correction reported by Ingebrethsen and Sears (1989). However, this information allows only approximate re-calibration of the OPC because the outputs of both OPC and EC cover a range of particle sizes instead of single size. OPC channel size limits were corrected for differences in refractive index by calculating the signal intensities of given ETS (refractive index 1.51, McRae, 1982) and PSL (refractive index 1.59) particle size with the Mie theory (Hinds, 1982).

A personal computer controlled the aerosol instruments and logged the data via a data-acquisition system (Keithley, Series 500). The EC was stepped through a 10 minute cycle of 14 voltages, each held for 40 seconds, with an additional 40 seconds added to the highest voltage step. After each change in EC voltage, some time was required for instrument output to stabilize. Therefore, particle concentration data were obtained only from the final 10 seconds of each voltage step by averaging 5 readings of the UCPC 2-second count buffer. OPC count data were logged at 2 minute intervals. The total particle concentration was recorded from the CNC every 30 seconds. Each experiment lasted for more than 20 hours.

The experiment was begun by initiating data acquisition from the aerosol instruments with the computer. All events after this point were computer controlled. The

HEPA filter air cleaner, which had been manually started prior to sealing the experimental room, was stopped after 30 minutes elapsed time. At that time, background total particle concentration in the room reached about 10 particles/cm^3. Cigarette smoking commenced at 60 minutes elapsed time. After the experiment, the remaining tobacco smoke was removed from the room with the exhaust hood. Data on background particles, collected by following the same procedure minus the cigarette, were used for estimating the outdoor particle infiltration.

Ventilation Rate

The ventilation rate was determined from the decay of SF_6 tracer gas concentration as monitored by a gas chromatograph (GC) with an electron capture detector (Hewlett Packard, Model 5890). In each experiment, 20-25 ml of 17.6% SF_6 in helium was injected into the room through a Polyflo tube in close proximity to the smoke plume. SF_6 was continuously drawn from the room through Norprene sample lines at three points, two in the room near floor and ceiling and a third directly from the particle sampling manifold. SF_6 measurements were concurrent with ETS particle measurements and continued for the duration of the experiment.

Flow Velocity

Measurements of air flow velocity with and without mixing fans operating were made in the room in a separate set of experiments. The normal particle sampling flow was withdrawn from the room to match conditions existing during ETS particle measurement. An omnidirectional air velocity probe (TSI, Model 8470) with a range of 0 to 30.5 m/s was attached to a stand. The signal from the probe was logged by the computer. Zero flow was measured by placing a 500 ml plastic bottle over the probe. To map the air velocity in the room, an experimenter fixed the probe at a preselected location in a 3-dimensional grid and exited the room. After allowing sufficient time for turbulence introduced by human activity to disappear (approximately 2-3 minutes from experimental observation), the probe signal was logged at 5 second intervals for a duration of 60 seconds. The probe was then

fixed at the next location and the process repeated. The room was divided into 60 elements with equal volumes, yielding a grid of 60 measurement points, with 5 divisions along the length axis, 4 along the width and 3 along the height.

RESULTS AND DISCUSSION

Coagulation Effect

Theoretically, the decay of a particle number concentration is first order, i.e., the decay rate is proportional to the number concentration, if the particles are removed only by deposition and ventilation. This is the case for the particles in the size range 0.43 to 0.54 μm diameter, shown in Figure 2. As seen, the decay curve after the first 100 minutes is a straight line on the semilog scale, suggesting first-order decay. In the first 100 minutes after cigarette ignition, the particle concentration decays much faster, probably due to dilution by the mixing in the room air (Baughman et al., 1993). Analyses of SF_6 concentration at three sampling locations show that complete mixing can be obtained in 50 to 100 minutes.

Careful observation of the decay curve for size range 0.267 to 0.322 μm reveals a slight increase in decay rate at about 1000 minutes. Analyses have shown that this variable decay rate is due to particle coagulation, which will be discussed later. The first order decay is not observed for the smaller particles (0.095 to 0.116 μm) shown in Figure 2. The particles with diameters in the range of 0.069 to 0.084 μm decay much faster than the other size classes, suggesting that they are removed not only by surface deposition and ventilation but also coagulation.

To correct for the particle coagulation effect, the change in number concentration due to coagulation was calculated for each measurement with the approach developed by Gelbard and Seinfeld (1980). The model was originally developed for mass concentration and has been modified for number concentration in this work. For a given particle size

range k, for which the mean size is d_k and the corresponding volume is v_k, the change in number concentration, n, due to coagulation can be calculated by

$$\begin{aligned}\frac{dn}{dt} = & \frac{1}{2}\sum_{i=1}^{k-1}\sum_{j=1}^{k-1}\theta(v_{k,L} < v_i + v_j < v_{k,U})\alpha(d_i,d_j)n(d_i,t)n(d_j,t) \\ & - \sum_{i=1}^{k-1}\theta(v_i + v_k > v_{k,U})\alpha(d_i,d_k)n(d_i,t)n(d_k,t) \\ & - \theta(2v_k > v_{k,U})\alpha(d_k,d_k)n(d_k,t)^2 \\ & - \frac{1}{2}\theta(2v_k < v_{k,U})\alpha(d_k,d_k)n(d_k,t)^2 \\ & - \sum_{i=k+1}^{m}\alpha(d_i,d_k)n(d_i,t)n(d_k,t)\end{aligned} \qquad (1)$$

where θ is the function which is equal to 1 if the specified condition is satisfied and 0 if it is not, α is the coagulation coefficient, d is particle size, v is particle volume, and t is time. The subscripts i, j, and k denote particle size ranges, and L and U denote the lower and the upper limits of a particle size range respectively. The first term on the right side of the equation considers the growth of the smaller particles to the particles in size range k. When a particle from size range k coagulates with a particle from a smaller or larger size range, it is removed from size range k if the volume of the newly formed particle is larger than $v_{k,U}$. The removal rate is given by the second and the fifth terms. The third and fourth terms are for the coagulation of the particles in the range k to form a particle larger and smaller than $v_{k,U}$, respectively. The coagulation coefficient was computed with the equation for particle collision by Brownian motion according to Seinfeld (1986).

The concentration changes resulting from coagulation were calculated based on the measured concentrations. Some of the results are depicted in Figure 3. It is shown that particle coagulation has a significant influence in the first 600 minutes after combustion, during which the total number concentration is greater than 10^4 particles/cm^3. Negative

changes indicate a decrease in particle number concentration. The loss rate for particles in the size range 0.069 to 0.084 μm is high in the first 200 minutes after cigarette combustion because of the high collision rate due to high number concentration. As the concentration of particles in this size range decays, the collision rate decreases and fewer particles are lost by coagulation, as indicated by the leveling-off of the curve. After 400 minutes, the curve adopts a slight positive slope, suggesting a small net production of these particles. A possible source of 0.069 to 0.084 μm particles is the coagulation growth of smaller particles.

For the size range 0.267 to 0.322 μm an increase in particle number concentration is observed until about 700 minutes after cigarette combustion. However, the concentration of particles in the range 0.43 to 0.54 μm shows negligible change. After 800 minutes all of the curves level-off, indicating negligible effects from particle coagulation. By this time, the total particle concentrations are generally lower than 8000 particles/cm^3. In summary, we found that coagulation leads to a decrease in the number of particles with diameters smaller than 0.25 mm and an increase in the number of particles between 0.25-0.5 μm while particles with a diameter larger than 0.5 μm (mean size for the size range 0.43-0.54 μm) show negligible change.

Ventilation Rate and Flow Turbulence Parameter

The measured ventilation rates fall in a narrow range of 0.017-0.02 ACH for the experiments at mixing fan speeds of 430, 2000, and 3070 rpm. SF_6 concentration data for the experiment with mixing fans off show an unstable ventilation rate of about 0.03 to 0.05 ACH, possibly due to the windy weather and poor mixing of the room air. Since the ventilation rates were stable in following three days of data collection, a ventilation rate of 0.02 ACH was used for this fan off experiment as well.

Particle deposition indoors depends on near-surface air flow characteristics which in turn depend on air motion in the core of the room and on surface-air temperature differences. The core air motion may be characterized by the intensity of the flow

fluctuation and an average velocity. Flow fluctuation can be produced by large-eddy shedding by furniture or other objects which create a flow blockage, non-uniform temperature of air and surfaces, and human activity. Studies of air flow in clean rooms have shown that flow fluctuations exist almost everywhere and are different from the high Reynolds number turbulent flow in pipes (Ye et al., 1991). It is believed that the room air flow exhibits unsteady laminar flow, weaker diffusion and dissipation of eddy energy, and larger scale. Typical air velocities in a room are also much lower than the velocity of turbulent flow in a pipe.

The particle deposition theory of Crump and Seinfeld (1981) assumes uniform turbulent flow in an enclosure. A parameter, K_e, is used to characterize the turbulent transport of particles through the boundary layer. According to Corner and Pendlebury (1951), K_e can be determined from the flow velocity gradient which is a function of average flow velocity, $\bar{u}$, and the length of the surface in the direction of flow, L, by

$$K_e = K_o^2 \frac{d\bar{u}}{dx} \qquad (2)$$

where x is the distance from the surface, $d\bar{u}/dx$ is the flow velocity gradient, and K_o is the Kármán turbulence constant. For fully turbulent flow in a pipe, K_o=0.4 and falls to a value near 0.2 on entering the transition region near the walls (Corner and Pendlebury, 1951). The velocity gradient is given by

$$\frac{d\bar{u}}{dx} = 0.037\left(\frac{\bar{u}^9 \rho^4}{\eta^4 L}\right)^{1/5} \qquad (3)$$

where ρ is the air density and η is air viscosity.

When mixing fans are off, air movement in the room is mainly natural convection, induced by the temperature differences between interior surfaces and room air. In this case, either the turbulent deposition model of Crump and Seinfeld (1981) or the natural convection model of Nazaroff and Cass (1989a) might describe deposition as a function of particle size. Our measurements with the air velocity probe show that the average natural convection flow velocity at 60 measurement points is 4.0 cm/s . The average velocity increases to 19 cm/s when the four mixing fans on the walls are running at full speed (3070 rpm). Velocity measurements in the rooms of a residential house yielded average flow velocities over a similar range: 4.2-15.5 cm/s (Matthews et al., 1989), indicating that the flow velocities for our experimental conditions are similar to the range of velocities in the residential house. We use the height of wall as the length of surface at the flow direction, L, in equation (3) for flow gradient. The specific choice of L is not important since K_e scales as $L^{-1/5}$. Since the room air flow might be more like the flow in the transition region, as indicated above, K_o=0.2 was chosen for the turbulence parameter calculations.

Table I shows the calculated turbulence parameters for two different flow conditions: (1) natural convective flow and (2) full speed mixing fan operation (3070 rpm). For the natural convection case, K_e is low (0.026 1/s), indicating weak turbulent mixing within the experimental room. Previous measurements indicated a temperature difference of about 0.3 ^{o}C between room air and surfaces at non-heating conditions, rising to 1.5 ^{o}C when there is incoming solar radiation through windows (Baughman et al., 1993). This difference is sufficient to induce natural convection in our experimental room according to Holländer et al. (1984).

When a fan is used to stir the air, mechanical energy is transferred from the fan to the air, eddies are generated and dissipate rapidly. As seen in Table I, K_e increases to 0.45 1/s at full fan speed, which is between the values reported for a 0.45 m^3 chamber at low and high fan speeds (Ingebrethsen and Sears, 1989).

Okuyama et al. (1986) successfully determined the turbulence parameter, K_e, with the power number and stirring speed of the propellers in a chamber. However, for the case of natural convection (fans off), K_e can not be determined with their technique. For a residential dwelling without controlled mixing as in laboratory studies, the turbulence parameter, K_e, can be roughly estimated, as here, with the equations (2) and (3) by measuring flow velocity within the dwelling.

Deposition Coefficient

According to Crump and Seinfeld (1981), the removal rate of particles by deposition is related to particle concentration by a deposition coefficient, β, through

$$\frac{dn}{dt} = -\beta n. \qquad (4)$$

The deposition coefficient accounts for the influences of particle size, flow turbulence, and orientation of a substrate surface. Mathematically, the value of β is the sum of β_w, β_c, and β_f, which represent the deposition coefficients for wall, ceiling, and floor, respectively. For the homogeneous turbulence model of Crump and Seinfeld, the deposition coefficients are related to the turbulence intensity, K_e, by

$$\beta_w = \frac{2S_w}{\pi V}\sqrt{DK_e} \qquad (5)$$

$$\beta_c = \frac{S_c}{V}\frac{v_g}{\exp\left(\frac{\pi}{2}\frac{v_g}{\sqrt{DK_e}}\right)-1}$$

$$\beta_f = \frac{S_f}{V} \frac{v_g}{1 - \exp(-\frac{\pi}{2} \frac{v_g}{\sqrt{DK_e}})}$$

where S_j is the respective area of the jth surface, V is the room volume, D is particle diffusivity, and v_g is particle settling velocity due to gravitation.

The measured particle concentrations with time were corrected for the effects of coagulation and ventilation, and then used to calculate the deposition coefficient for each size range with equation (4). The results for four mixing fan conditions are shown in Figure 4. The uncertainties in the calculated deposition coefficients shown in Figure 4 are based on the variability of particle concentration. The effects of imperfect mixing and variable particle infiltration are not considered.

For a given K_e, β depends on particle diffusivity, D, and gravitational settling velocity, v_g. When a particle is small enough, D dominates the change of β with particle size. D increases as particle size becomes smaller, resulting in an increase in deposition coefficient, β. For a large particle, however, the effect of v_g on β may overwhelm the effect of diffusivity, D, and β increases as particle size increases. The overall dependence of β on particle size can be seen in Figure 4. A minimum deposition coefficient will be found when neither D nor v_g dominates the change in β. For the natural convection flow, or zero mixing fan speed, the smallest β is found for particles with diameters between 0.1 to 0.2 μm. At full mixing fan speed (3070 rpm), the smallest β is found for particles in size range 0.2 to 0.3 μm.

Equations (4) and (5) were used to estimate the turbulence parameter, K_e, by fitting the experiment data, represented by the solid lines in Figure 4. Thus these solid lines represent a theoretical fit with one free parameter, K_e. Even though the theoretical curve does not go through all of the data, the data and the theory show similar trends. The

measurements for particles with diameters between 0.1 and 0.2 μm give a smaller β than the theory at the four mixing conditions. This might be due to the non-uniform turbulence, imperfect mixing, and variable particle infiltration in the experimental room. Note that the experimental results for 0.1 μm<d_p<0.2 μm are very sensitive to the measured value of air exchange rate. Although the reported results represent our best determination of β, the values have an uncertainty of the order of 10^{-6} 1/s.

For particles larger than 0.6 μm, the deposition coefficients obtained from experimental measurements are more strongly dependent on the air mixing condition than the theory predicts, as shown in Figure 4. It is possible that additional deposition occurs on the moving fan blades. For large particles, moreover, inertial effects may become significant at high particle velocity (e.g. near to fans). When the particles approach a surface, they may inertially enter the boundary layer and deposit on the surface.

The estimated turbulence parameters listed in Table I were also used with equations (4) and (5) to calculate the deposition coefficients. As shown in Figure 5, The experimental data do not agree well with the prediction for particles with diameters in the range 0.1 to 0.2 μm at two mean air velocities and for particles larger than 0.6 μm at fan speed 3070 rpm. As discussed above, we may attribute these differences to the approximations of uniform turbulence, the possible additional deposition on fan blades, and neglect of inertial effect.

The experimental data for the natural convection flow (no mixing fan operating) were also compared with model predictions of Nazaroff and Cass (1989a). As surface-air temperature differences were not measured during the experiments, earlier work by Baughman et al (1993) in the same space shows that the expected magnitude of the temperature differences is 0.3 ^{o}C. Figure 6 shows that the model predictions conform well with the data for $d_p \geq 0.1$ μm, particularly for $T_s - T_{air} = -1$ ^{o}C.

Deposition Rate Prediction

We have used Crump and Seinfeld's theory with the experimentally estimated parameters to predict ETS particle deposition under selected environmental conditions. The calculations include effects of coagulation and ventilation. The room air is assumed to be uniformly turbulent with a parameter K_e=0.026 1/s representing the natural convection. An air exchange rate of 0.02 ACH is used. The particles initially (i.e. at 1 hour after combustion) have a lognormal distribution with geometric mean diameter d_g=0.14 μm, geometric standard deviation σ_g=1.83, and total number concentration 3.68×10^4 particles/cm^3, based on the experimental measurements in the fan-off condition. The predicted time-integrated deposition as a function of particle size is shown in Figure 7 after a 10 hour period following smoking of one cigarette. For comparison, the airborne particle size distributions are shown for the period immediately following cessation of smoking (assuming well-mixed conditions) and 10 hours later. Particle number is used instead of concentrations in this figure to facilitate comparison between the deposited and airborne particles.

The small and large particles deposit more rapidly than midsize particles due to the high Brownian diffusivity and the high settling velocity, respectively. After 10 hours, more of the particles with diameters larger than 0.95 μm and between 0.026 to 0.069 μm have deposited on the surfaces than remain airborne (Fig. 7). Most particles with diameters between 0.069 and 0.95 μm remain in suspension. For particles smaller than 0.026 μm, the number remaining airborne is larger than that deposited. This may be explained by an increase in suspended particles by infiltration. Integrating the deposition distribution shows that 10% by number of sidestream ETS particles have deposited on the interior surfaces at 10 hours after smoking one cigarette in the 4.58 by 3.38 by 2.37 m room with a low ventilation rate.

The mass of deposited particles was calculated for three different ventilation rates and the results are shown in Figure 8. Although a higher turbulence intensity may possibly

accompany a higher ventilation rate, we have assumed a constant intensity with K_e=0.026 1/s for the three ventilation rates of 0.03, 0.5, and 1 ACH. At the higher ventilation rates, ETS particles are removed more efficiently by ventilation and the indoor particle concentration is diluted by infiltrating air with lower particle concentrations. Therefore, fewer particles deposit on surfaces due to the lower concentration. Since small particles are entrained into the room, which are determined by the background measurements, their concentration may increase as ventilation rate increases, and therefore, more small particles deposit on the surfaces, as seen in the left tails of three deposition curves in Figure 8. Since the amount of deposition depends on particle concentration and size, as anticipated, the peak values for the deposited mass at three ventilation rates are for particles with diameters near 0.7 μm instead of 0.3 μm, the peak mass at the initial time shown in Figure 8. At an air-exchange rate 0.03 ACH, 21.5% of the total initial mass of 12 mg of the sidestream ETS particles generated by smoking one cigarette is estimated to deposit on the interior surfaces after 10 hours, which is equivalent to an average deposition rate of 0.02 1/hr. When the ventilation rate is increased by a factor of 15 to 0.5 ACH, 5.7% of the total mass will deposit. At 1 ACH, 3% is estimated to deposit on the surfaces. The estimated surface mass density of 10 $\mu g/m^2$ ETS particles is found on interior surfaces at 0.5 ACH, 10 hours after one cigarette is combusted.

Based on the data in Benner et al. (1989), we estimate an average evaporation rate of 17% per hour for ETS particles deposited on an indoor surface. Using this value and the deposition rate constant above, we estimate that at 0.02 ACH, re-emissions from deposited particles can yield indoor concentration of chemicals 100 $\mu g/m^3$ in 10 hours after smoking one cigarette This emission contribution of deposited particles will become more significant when more cigarettes are smoked and more particles deposit on the interior surfaces.

CONCLUSIONS

Airborne tobacco smoke particles undergo coagulation, deposition, and removal by ventilation. The observed ETS particle concentration decays at different rates for different particle sizes. Since the smaller particles coagulate to form larger particles, the number concentration of smaller particles decays faster than that for the larger particles. With our experimental conditions, the particles smaller than 0.25 μm diameter are removed by coagulation to form larger particles with diameter between 0.25 and 0.5 μm. The effect of coagulation on the concentration of particles larger than 0.5 μm was found to be negligible. When the particles are removed or diluted to a total number concentration of less than about 8000 particles/cm^3, coagulation is not significant for any particle size.

ETS particle deposition on interior surfaces has been determined from particle concentration measurements by correcting for the effects of coagulation and ventilation. Air turbulence has been estimated with the measured air velocities and the length of surface in the direction of flow. It showed that both the experimental data and the predictions with Crump and Seinfeld's homogeneous turbulence theory and Nazaroff and Cass' natural convection theory have the similar dependence on particle size. However, the theoretical curves do not agree thoroughly with the experimental data. The disagreement between the measurements and the theory may be attributed to the non-uniform turbulence, imperfect mixing, and variable particle infiltration.

A significant amount of ETS particles may deposit on the interior surfaces at the normal ventilation rate of a residence. These deposited particles might be a secondary source of indoor air pollutants. Increasing the ventilation rate can reduce ETS particle concentrations in a room, and therefore, decrease the deposition rate. However, an optimum ventilation condition for a home of smokers should be chosen by considering energy conservation and health effects.

REFERENCES

Badre, R., Guillerm, R., Abran, N., Bourdin, M., and Dumas, C. (1978). Ann. Pharm. Fr. 36:443-452.

Baughman, A.V., Gadgil, A.J., and Nazaroff, W.W. (1993). Submitted to Indoor Air.

Benner, C.L., Bayona, J.M., Caka, F.M., Tang, H., Lewis, L., Crawford, J., Lamb, J.D., Lee, M.L., Lewis, E.A., Hansen, L.D., and Eatough, D.J. (1989). Environ. Science Technol. 23:688-699.

Chen, B.T., Yeh, H.C., and Cheng, Y.S. (1992). Aerosol Sci. Technol. 17:9-24.

Corner, J., and Pendlebury, E.D. (1951). Proc. Phys. Soc. B64:645-654.

Crump, J.G., Flagan, R.C., and Seinfeld, J.H. (1983). Aerosol Sci. Technol. 2:303-309.

Crump, J.G., and Seinfeld, J.H. (1981). J. Aerosol Sci. 12:405-415.

Eatough, D.J., Benner, C.L., Bayona, J.M., Richards, G., Lamb, J.D., Lee, M.L., Lewis, E.A., and Hansen, L.D. (1989a). Environ. Science Technol. 23:679-687.

Eatough, D.J., Hansen, L.D., and Lewis, E.A. (1989b). In Environmental Tobacco Smoke: Proceedings of the International Symposium at McGill University 1989; Ecobichon, D.J.; Wu, J.M., Eds; pp 3-39, Lexington Books, D.C. Health and Company, Lexington, KY.

Gelbard F., and Seinfeld, J.H. (1980). J. Colloid Interface Sci. 78:485-501.

Hinds, W.C. (1982) Aerosol Technology: Properties, Behavior, and Measurement of Airborne Particles John Wiley & Sons, Inc., New York.

Holländer, W., Hehnke, W., Koch, W., and Pohlmann, G. (1984). In Proceedings of 3rd European Symposium Physico-Chemical Behavior of Atmospheric Pollutants, Versino B. and Angeletti, G. Eds., pp.309-319, D. Reidel, Dordrecht.

Ingebrethsen, B.J., and Sears, S.B. (1989). J. Colloid Interface Sci. 131:526-536.

Ligocki, M.P., Liu, H.I.H., Cass, G.R., and John, W. (1990). Aerosol Sci. Technol. 13:85-101.

Matthews, T.G., Thompson, C.V., Wilson, D.L., Hawthorne, A.R., and Mage, D.T.

(1989). Environ. Int. 15:545-550.

McMurry, P.H., and Grosjean, D. (1985). Environ. Sci. Technol. 19:1176-1182.

McRae, D.D. (1982). J. Colloid Interface Sci. 87:117-123.

National Research Council, Committee on Passive Smoking Board on Environmental Studies and Toxicology (1986). Environmental Tobacco Smoke: Measuring Exposures and Assessing Health Effects. National Academy Press, Washington, D.C.

Nazaroff, W.W., and Cass, G.R. (1989a). Environ. Int. 15:567-584.

Nazaroff, W.W., and Cass, G.R.(1989b). Environ. Sci. Technol. 23:157-166.

Nazaroff, W.W., Ligocki, M.P., Ma, T., and Cass, G.R. (1990). Aerosol Sci. Technol. 13, 332-348.

Nelson, P.R., Heavner, D.L., Collie, B.B., Maiolo, K.C., and Ogden, M.W. (1992). Environ. Science Technol. 26:1909-1915.

Offermann, F.J., Sextro, R.G., Fisk, W.J., Grimsrud, D.T., Nazaroff, W.W., Nero, A.V., Revzan, K.L., and Yater, J. (1985). Atmos. Environ. 19:1761-1771.

Okuyama, K., Kousaka, Y., Yamamoto, S., and Hosokawa, T. (1986). J Colloid Interface Sci. 110:214-223.

Pandian, M.D., and Friedlander, S.K.(1988). PCH PhysicoChemical Hydrodynamics 10, 639-645.

Seinfeld, J.H. (1986). Atmospheric Chemistry and Physics of Air Pollution John Wiley & Sons, Inc., New York.

Sexton, K., Webber, L.M., Hayward, S.B., and Sextro, R.G. (1986). Environ. Int. 12:351-362.

Turner, S., Cyr, L., and Gross, A.J. (1992). Environ. Int. 18:19-28.

US EPA (1993). Respiratory Health Effects of Passive Smoking: Lung Cancer and Other Disorders, EPA/600/6-90/006F.

Ye, Y., Pui, D.Y.H., Liu, B.Y.H., Opiolka, S., Blumhorst, S., and Fissan, H. (1991). J. Aerosol Sci. 22:63-72.

Table I. Average flow velocities and turbulence parameters

	natural convection	high fan speed (3070 rpm)
$\bar{u}$, cm/s	4.0	19
standard deviation	0.16	0.78
number of measurement locations	60	60
$d\bar{u} / dx$, 1/s	0.66	11.26
K_e, 1/s	0.026	0.45

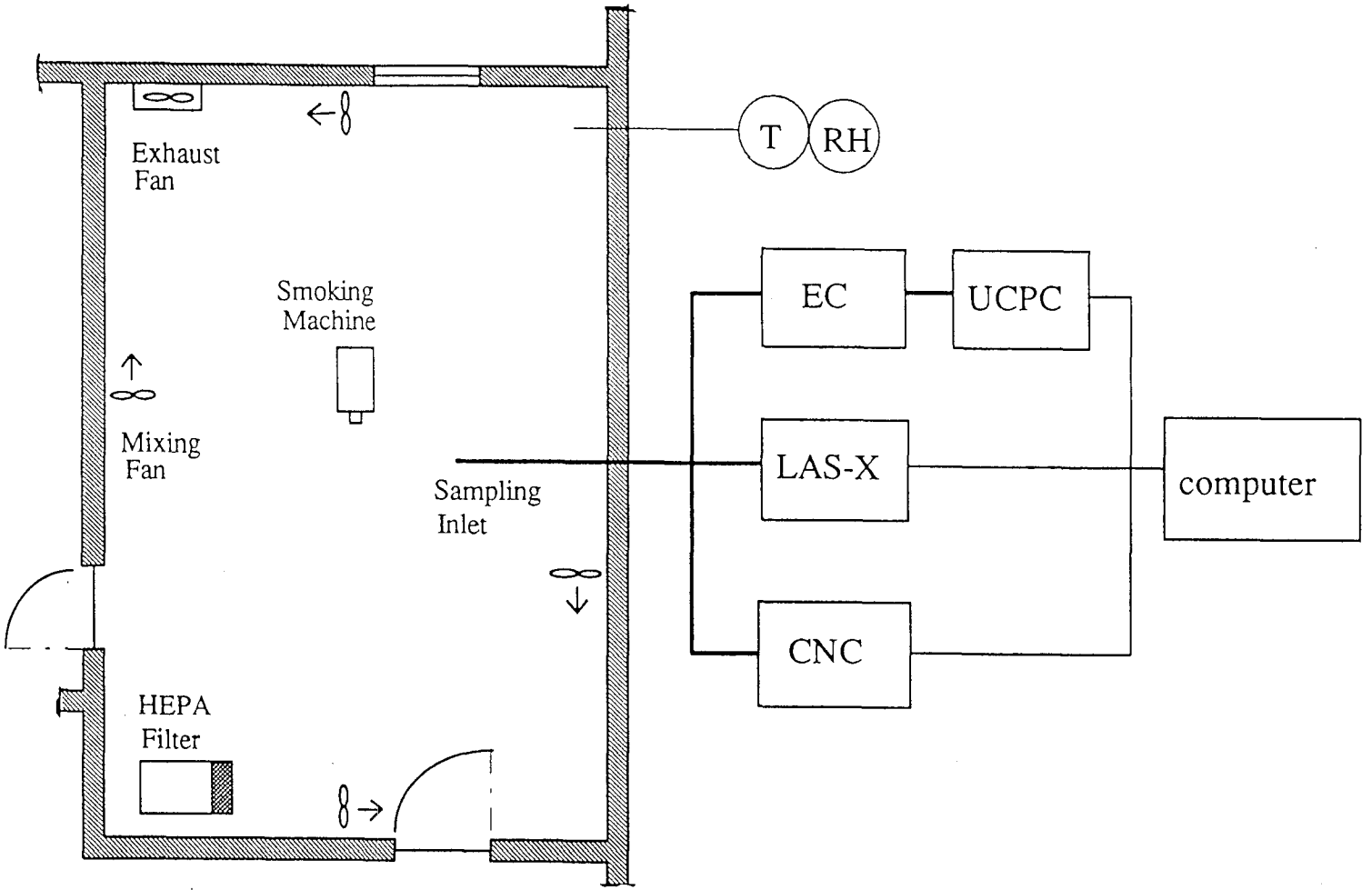

Figure 1. Schematic drawing of the experimental room and measurement system. The room located in a two floor building has a size of 4.56x3.38x2.37 m high. T= temperature probe; RH=relative humidity probe; EC=electrostatic classifier; UCPC=ultrafine condensation particle counter; LAS-X=laser aerosol spectrometer; CNC=condensation nucleus counter. The arrows show the fan driven air flow direction.

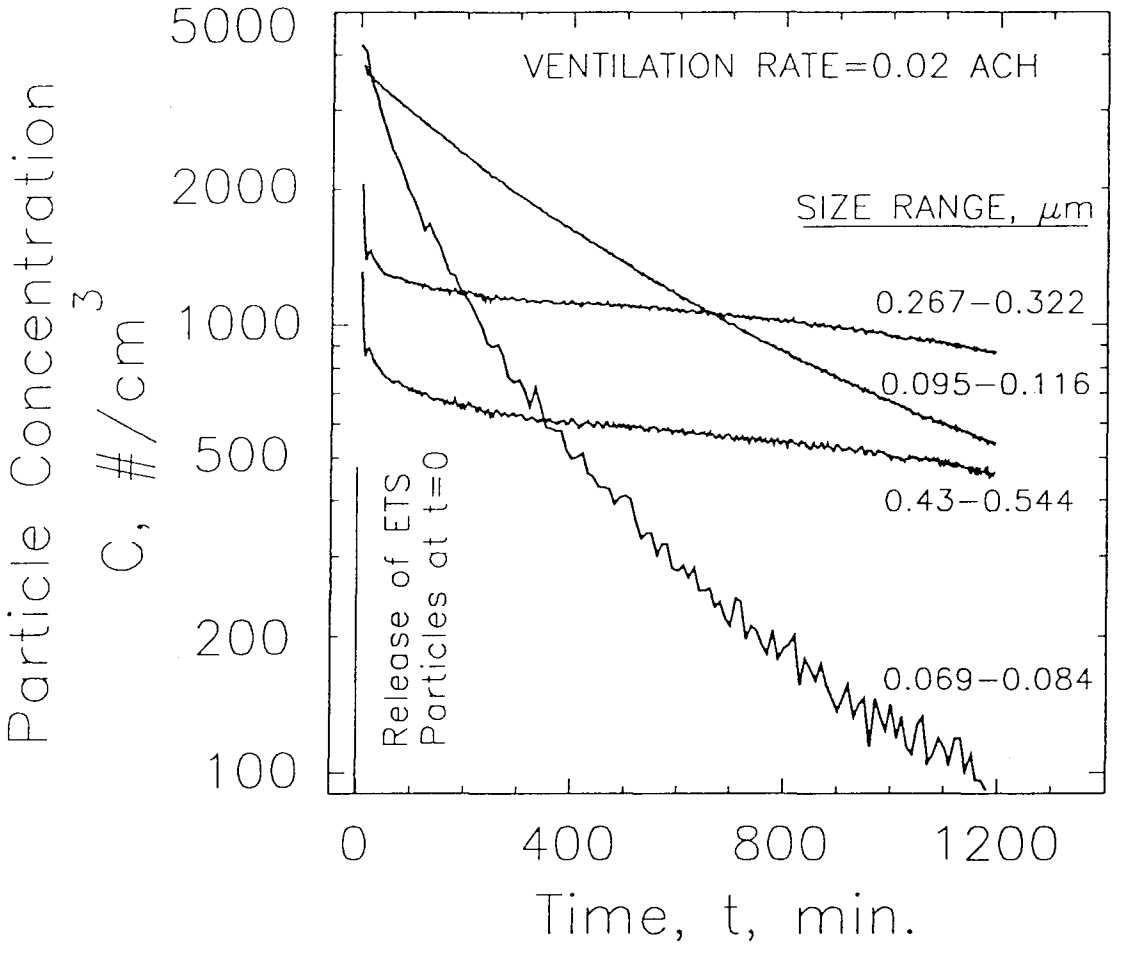

Figure 2. Measured decrease in particle number concentration with time. The measurement data on particles with diameters >0.095 μm were obtained with the OPC and the smaller particles with EC+UCPC.

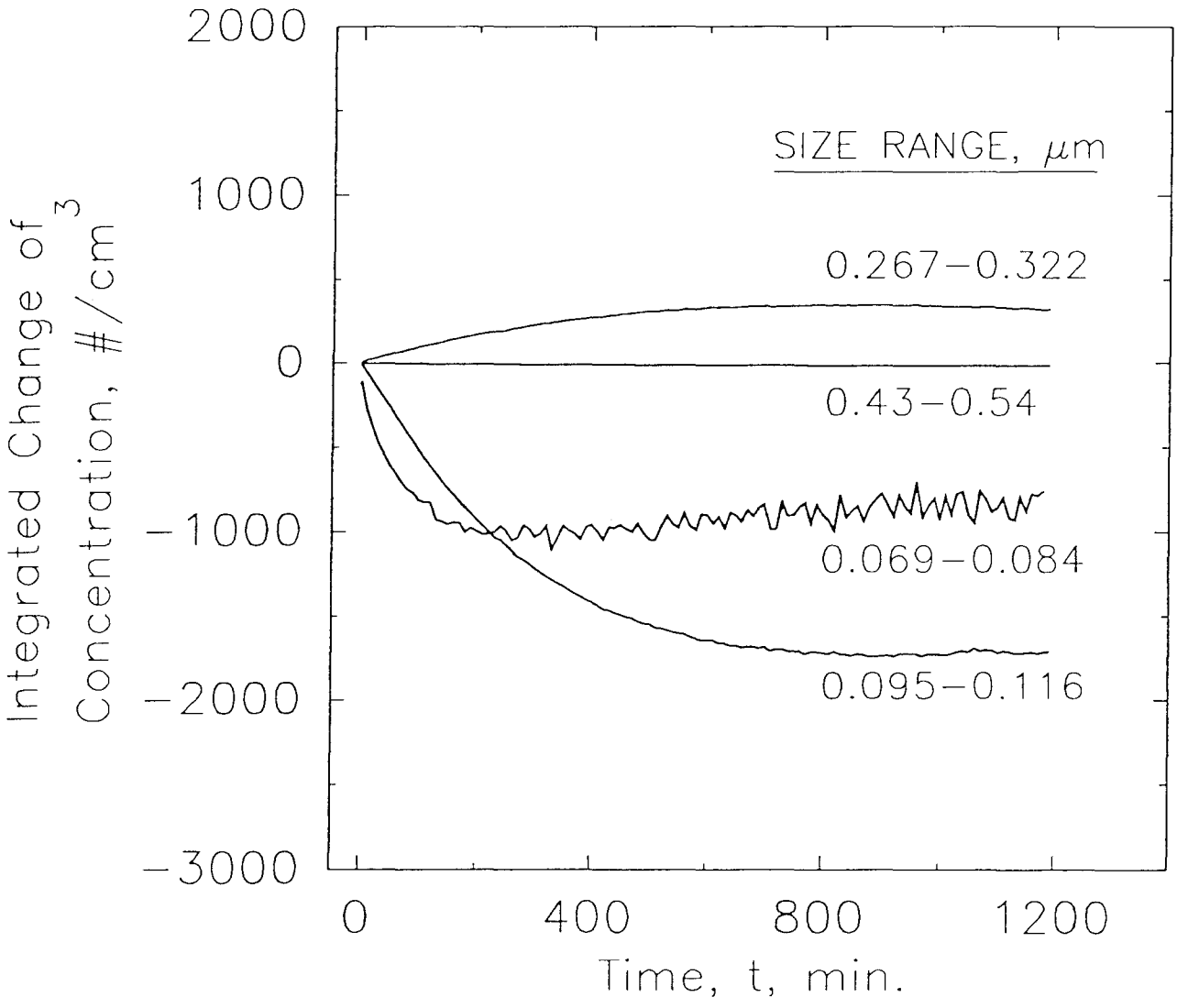

Figure 3. The calculated change in ETS particle concentrations for selected size ranges due to coagulation under the experimental conditions.

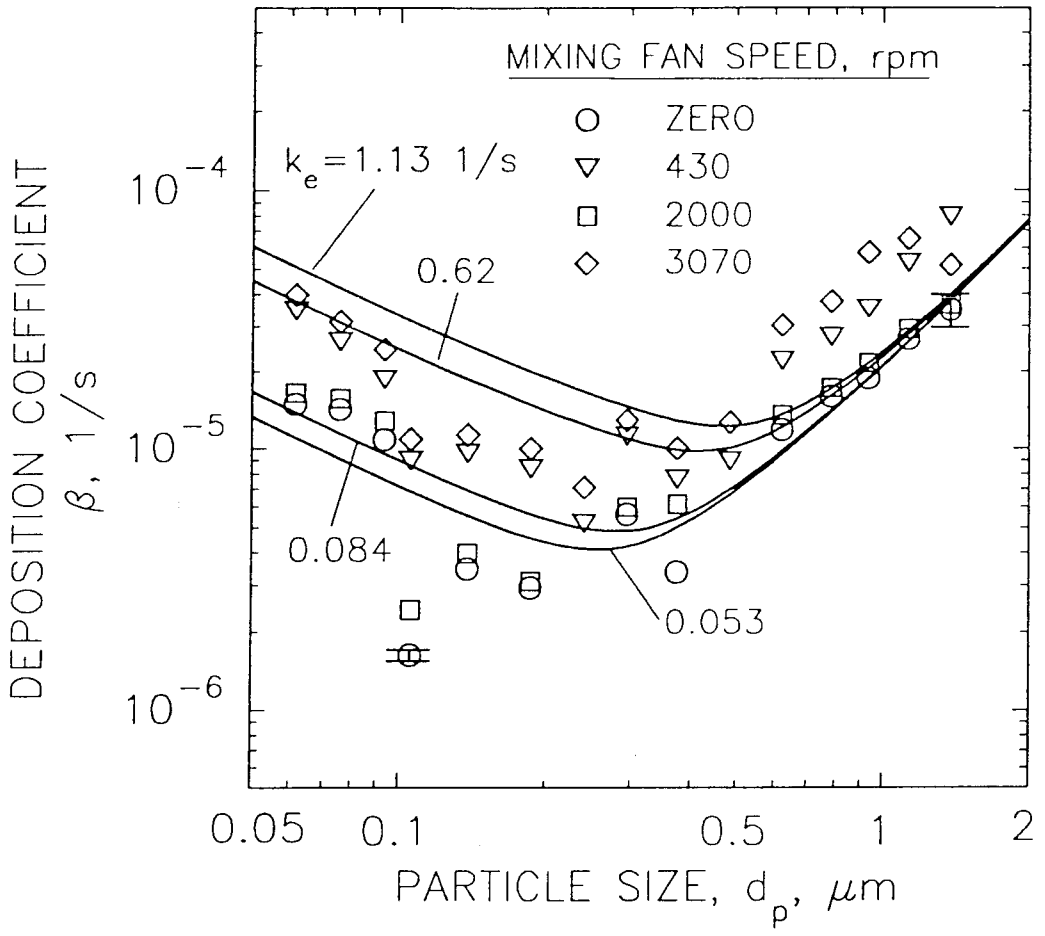

Figure 4. Particle deposition coefficient for different mixing rates. The data points were obtained by correcting the experimental results for coagulation and ventilation effects. The solid lines are based on Crump & Seinfeld's homogeneous turbulence theory (1981) for the indicated values of K_e, and represent the best fits to the experimental data.

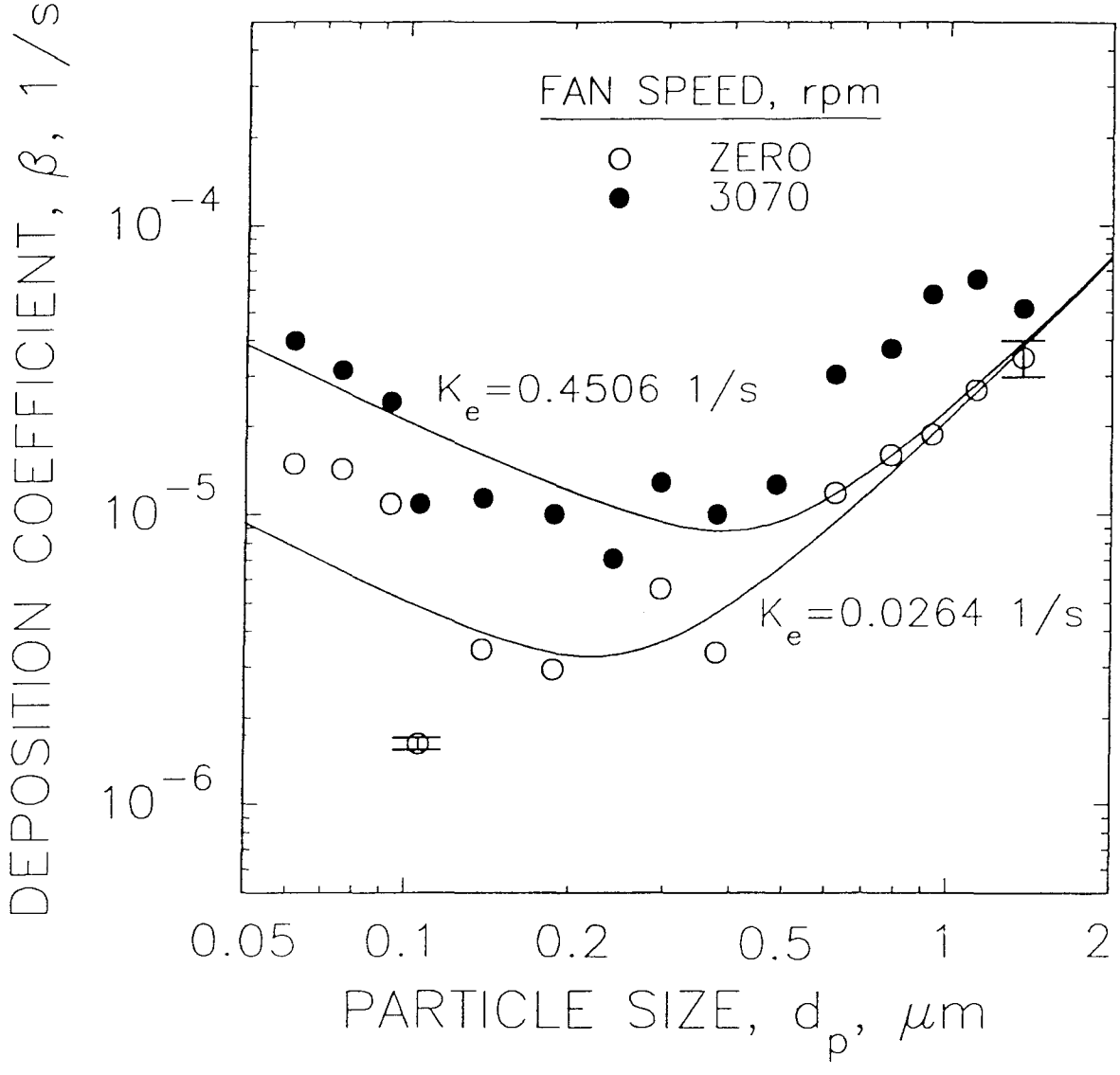

Figure 5. Deposition coefficients for both natural flow and high mixing fan speed. The data points were obtained by correcting the experimental results for the effects of coagulation and ventilation. The solid lines are the calculations with Crump & Seinfeld's homogeneous turbulence theory (1981) by using the K_e estimated based on the measured data.

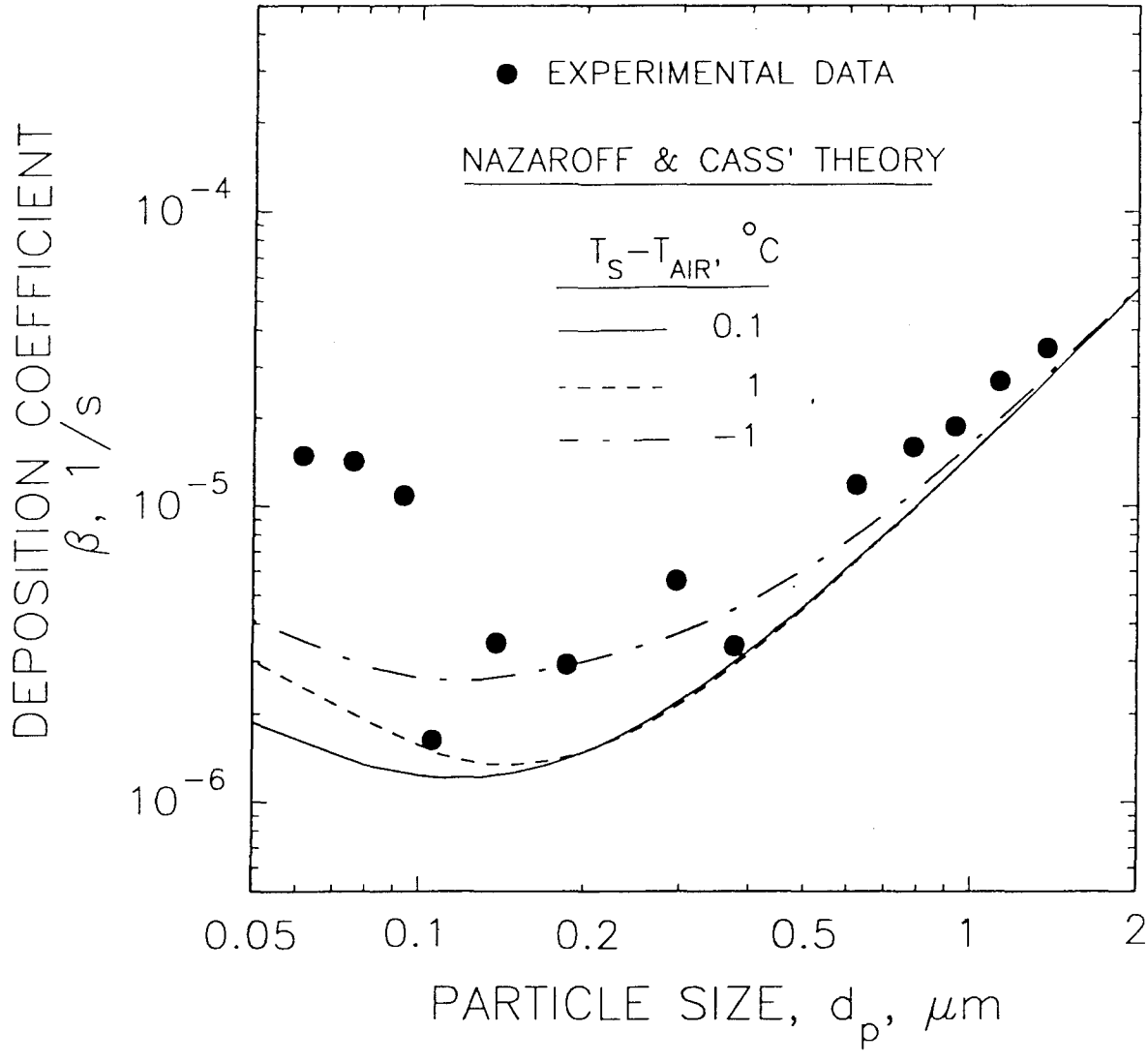

Figure 6. Comparison of experimental data on deposition coefficient vs. particle diameter with model predictions for natural convection flow (Nazaroff & Cass, 1989a). Data are for fan-off condition only. Model predictions are presented for three different surface-air temperature differences, T_S-T_{air}. In each case, temperature is assumed constant over all surfaces.

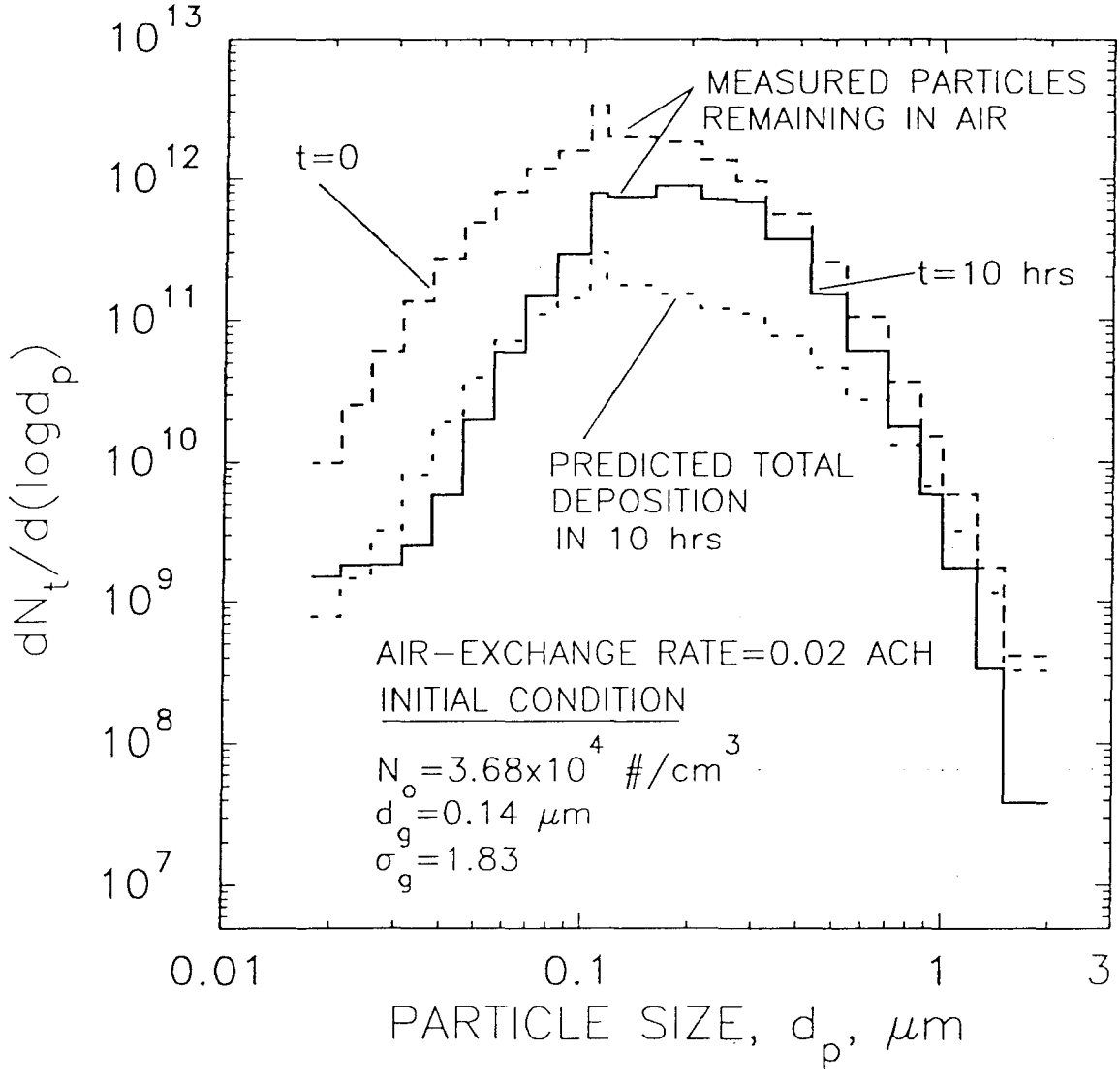

Figure 7. The predicted particle deposition on interior surfaces compared with measured particle numbers suspended in room air as a function of particle size. The air flow is assumed to be uniformly turbulent with a parameter K_e=0.026 1/s (fan off). N_t=total particle number.

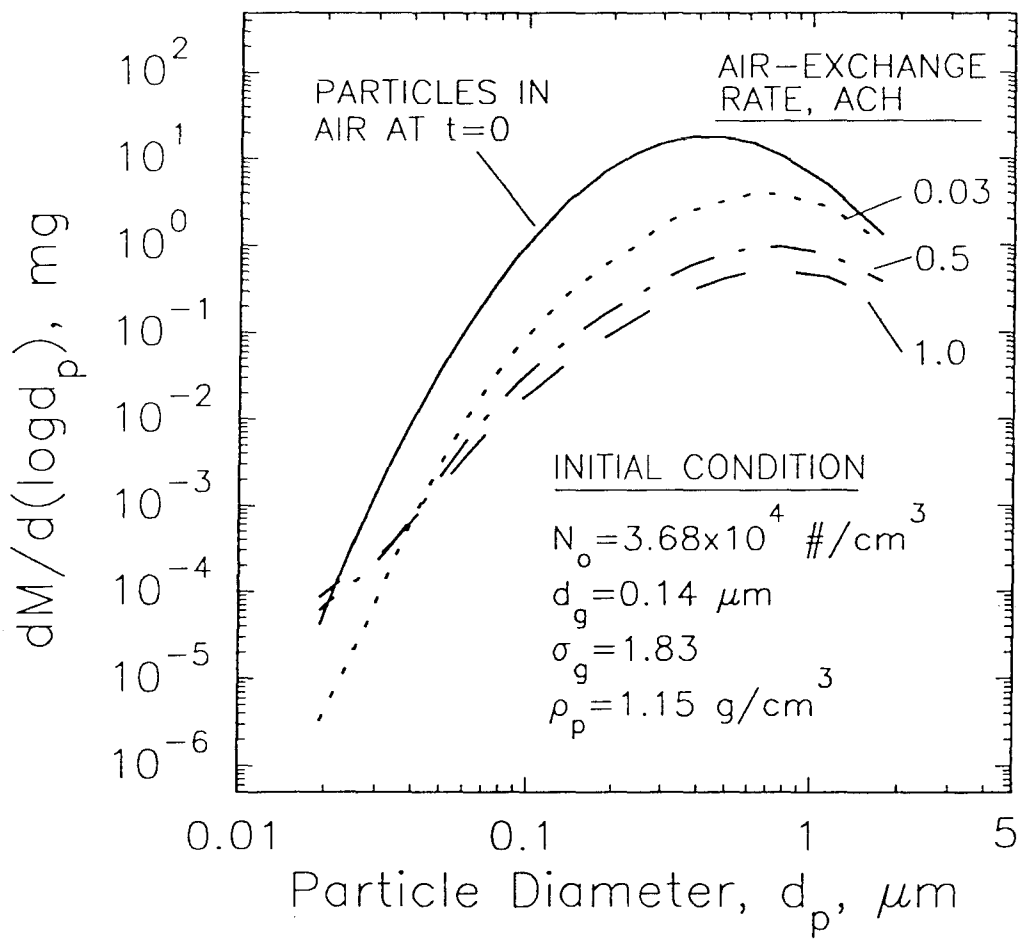

Figure 8. The total mass of the particles deposited on the interior surfaces in 10 hours after burning a cigarette. The turbulence intensity for room air is considered to be constant (K_e=0.026 1/s) for the differing ventilation rates. The initial airborne particle mass distribution (1 hour after ignition) is shown for comparison.